

## RESEARCH ARTICLE

# Examination of SOD1 aggregation modulators and their effect on SOD1 enzymatic activity as a proxy for potential toxicity

Ravinder Malik<sup>1</sup> | Christian Corrales<sup>1</sup> | Miriam Linsenmeier<sup>1</sup> | Huda Alalami<sup>1</sup> | Niki Sepanj<sup>1</sup> | Gal Bitan<sup>1,2,3</sup>

<sup>1</sup>Department of Neurology, David Geffen School of Medicine at UCLA, University of California at Los Angeles, Los Angeles, CA, USA

<sup>2</sup>Brain Research Institute, University of California at Los Angeles, Los Angeles, CA, USA

<sup>3</sup>Molecular Biology Institute, University of California at Los Angeles, Los Angeles, CA, USA

## Correspondence

Gal Bitan, Gordon Neuroscience Research Building 451, Charles E. Young Drive South, Los Angeles, CA 90095.  
Email: gbitan@mednet.ucla.edu

## Present address

Miriam Linsenmeier, Department of Chemistry and Applied Biosciences, Institute for Chemical and Bioengineering, ETH Zurich, Vladimir-Prelog-Weg 1-5/10, Zurich, 8093, Switzerland

## Funding information

HHS | NIH | National Institute on Aging (NIA), Grant/Award Number: R01AG050721; RGK Foundation, Grant/Award Number: 20143057

## Abstract

Small-molecule inhibitors of abnormal protein self-assembly are promising candidates for developing therapy against proteinopathies. Such compounds have been examined primarily as inhibitors of amyloid  $\beta$ -protein ( $A\beta$ ), whereas testing of inhibitors of other amyloidogenic proteins has lagged behind. An important issue with screening compound libraries is that although an inhibitor suitable for therapy must be both effective and nontoxic, typical screening focuses on efficacy, whereas safety typically is tested at a later stage using cells and/or animals. In addition, typical thioflavin T (ThT)-fluorescence-based screens use the final fluorescence value as a readout, potentially missing important kinetic information. Here, we examined potential inhibitors of superoxide dismutase 1 (SOD1) using ThT-fluorescence including the different phases of fluorescence change and added a parallel screen of SOD1 activity as a potential proxy for compound toxicity. Some compounds previously reported to inhibit other amyloidogenic proteins also inhibited SOD1 aggregation at low micromolar concentrations, whereas others were ineffective. Analysis of the lag phase and exponential slope added important information that could help exclude false-positive or false-negative results. SOD1 was highly resistant to inhibition of its activity, and therefore, did not have the necessary sensitivity to serve as a proxy for examining potential toxicity.

## KEYWORDS

Proteinopathies, amyloid, enzyme activity, Thioflavin T, therapeutic index

## 1 | Introduction

Proteinopathies are diseases in which proteins self-assemble abnormally into cytotoxic oligomers and aggregates. Examples of proteinopathies include Alzheimer's disease, Parkinson's Disease, Huntington's Disease, and transthyretin amyloidoses involving aggregation of amyloid  $\beta$ -protein

( $A\beta$ ) and tau,  $\alpha$ -synuclein, huntingtin, and transthyretin, respectively (1). There are currently no disease-modifying therapies for most proteinopathies (2). In each disease, the aberrant protein(s) oligomers and amyloid fibrils can lead to cellular dysfunction and death (3). Therefore, discovery of compounds that can prevent and/or reverse the formation of these toxic assemblies is an attractive strategy for developing

Ravinder Malik and Christian Corrales contributed equally to the work.

© 2020 Federation of American Societies for Experimental Biology

therapies against proteinopathies (4). However, whereas this strategy has been explored extensively for Alzheimer's disease, primarily focusing on inhibitors of A $\beta$  aggregation and oligomerization (5), far fewer examples exist in the literature of testing small molecules as inhibitors of other amyloidogenic proteins. An important consideration in efforts to discover drug candidates based on this strategy is that such compounds must have a sufficient therapeutic index (TI), which typically means that the ratio of half-maximal lethal dose (LD<sub>50</sub>) or toxic dose (TD<sub>50</sub>) should be 100-1,000-times higher than the half-maximal efficacious dose (ED<sub>50</sub>).

Ideally, both the efficacy of aggregation inhibition and the compound's potential toxicity would be tested in parallel during the initial screening. In practice, however, the capability of compounds to inhibit aggregation often is screened initially *in vitro* whereas toxicity is tested in later steps in cell culture and/or animal models. Due to the significant expense and time required for such screening efforts, particularly if compounds are found to be toxic at relatively late stages, we asked if a simpler *in vitro* system could be developed for parallel testing of aggregation inhibition and toxicity. In principle, such a system could be developed if an essential functional property of an aggregation-prone protein could be used, inhibition of which would serve as a proxy for cellular toxicity. Measuring a compound's potential to inhibit the protein's function in parallel to testing the ability of the same compound to inhibit its aggregation would provide a convenient combined toxicity-efficacy screen *in vitro*. However, many amyloidogenic proteins, especially those involved in the major proteinopathies, such as, A $\beta$ , tau, and  $\alpha$ -synuclein, do not have an easily measurable function that can be tested *in vitro*. In contrast, the enzyme superoxide dismutase 1

(SOD1) has an easily measured essential activity—elimination of superoxide radical anions. Therefore, we chose SOD1 here as a potentially convenient system for testing this strategy (Figure 1).

SOD1 exhibits a gain of toxic function when mutations in the gene cause destabilization of the protein structure leading to formation of neurotoxic oligomers and aggregates in familial amyotrophic lateral sclerosis (fALS) (6). SOD1 is found normally in mitochondria where it converts superoxide radical anions, formed as a byproduct of mitochondrial respiration, into less toxic hydrogen peroxide (7). Subsequently, hydrogen peroxide is converted into water and oxygen by catalase. If a potential aggregation inhibitor were to prevent the function of SOD1, it would lead to a buildup of highly cytotoxic superoxide radical anions. Thus, the absence of SOD1 in homozygous SOD1-null mice leads to accelerated muscle loss and weakness (8) and yeast cells lacking SOD1 have disrupted metabolism, evidenced by a slower growth in early stages of culture followed by a complete halt of growth (9). Furthermore, a proposed mechanism for lead poisoning is through inhibition of SOD1 antioxidant activity leading to the accumulation of reactive oxygen species (10).

The enzymatic activity of SOD1 can be quantified indirectly using a colorimetric assay that measures the reduction of the colorless tetrazolium salt sodium 3'-[1-[(phenylamino)-carbonyl]-3,4-tetrazolium]-bis(4,6nitro)benzene-sulfonic acid (XTT) to a colored formazan (11). In this assay, the substrate for SOD1, the superoxide radical anion, is produced by the enzymatic reaction between xanthine oxidase and hypoxanthine (12) (Figure 2). When SOD1 is active, it reacts with the superoxide radical anions to produce hydrogen peroxide, preventing the reaction of the superoxide radical anions with

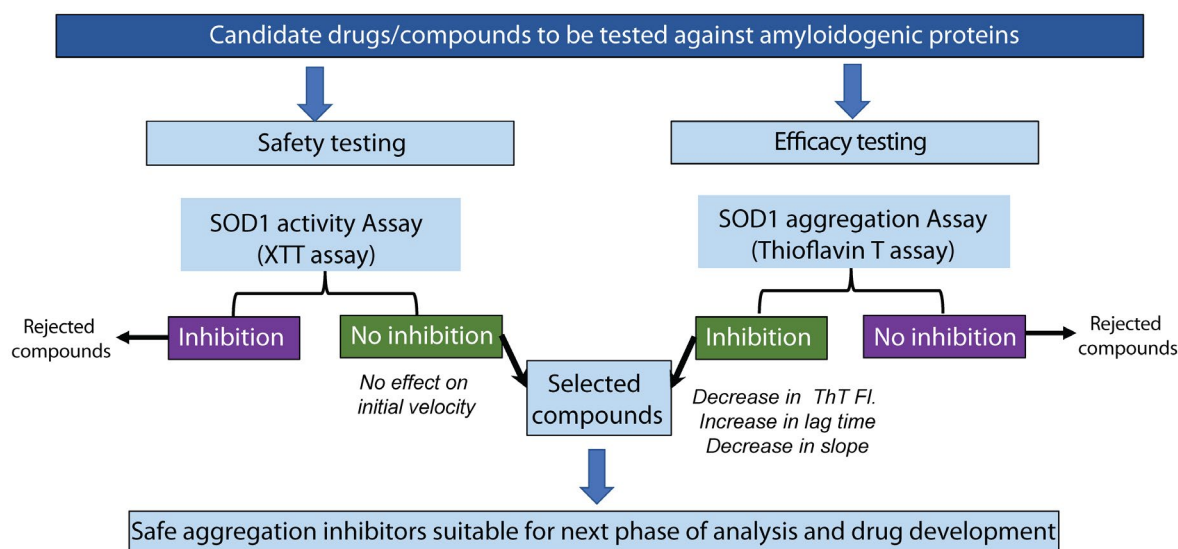


**FIGURE 1** Design of the parallel *in vitro* efficacy/toxicity screen. Safety testing examines the compounds for inhibition of SOD1 activity using the XTT assay. Compounds that inhibit the activity assay are rejected. Efficacy testing examines the compounds in parallel for inhibition of SOD1 aggregation using the ThT-fluorescence assay. Successful compounds are those that test negative for toxicity and positive for efficacy.

## Superoxide Dismutase 1 Activity Assay Reactions

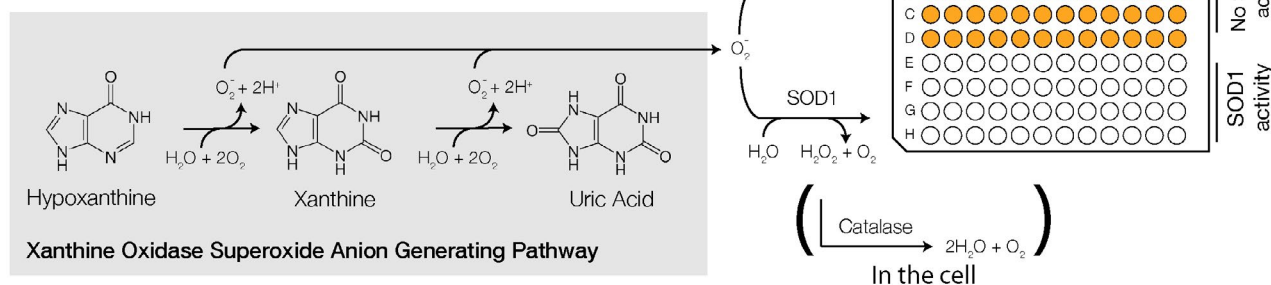


**FIGURE 2** A schematic representation of the safety assay. Hypoxanthine is converted by xanthine oxidase into a superoxide radical anion, which serves as a substrate for SOD1. Active SOD1 converts the superoxide radical anion into hydrogen peroxide, which in the cell is further reduced into water and oxygen by catalase. In the *in vitro* assay, inhibition of SOD1 allows the superoxide radical anion to react with XTT and convert it into an orange formazan dye, which can be quantified in typical multi-well plates.

XTT and leaving a colorless solution (Figure 2). If the activity of SOD1 is inhibited, the superoxide radical anions reduce XTT to the orange formazan. The absorbance of the formazan is directly proportional to the fraction of inactive SOD1 in the reaction (11).

Wild-type (WT)-SOD1 has an unusually high thermal stability and is resistant to denaturation (13). However, mutations in the cognate SOD1 gene lead to amino acid substitutions yielding SOD1 variants that are prone to misfolding and aggregation (7), which can be easily monitored using the thioflavin T (ThT) fluorescence assay (14). ThT is an amyloid-binding dye that shows increased fluorescence upon binding to the cross- $\beta$  structure of amyloid fibrils. The final fluorescence level is thought to correlate directly with the amount of amyloid fibrils formed, and therefore, has been used for screening of potential aggregation inhibitors, although this strategy is prone to artifacts. For example, competition between ThT and a potential inhibitor for the same binding sites or quenching of ThT fluorescence by the test compound would lead to a false-positive result. Contrarily, interaction between the test compound and ThT that would force ThT into planarity, thereby increasing the measured fluorescence, can lead to a false-negative result. Another complication is the stochastic nature of the aggregation reaction, which in the case of SOD1 has been shown by several studies to be an intrinsic feature causing the kinetics to vary substantially (15-18), which also may lead to false results in a screen if the majority of the replicates fail to yield a substantial increase in fluorescence during the time of the assay. Here, we tested several compounds previously reported to inhibit the aggregation of other proteins for their potential inhibition of SOD1 using the ThT assay. To account for the potential issues mentioned above, we analyzed separately the different phases of the sigmoidal curve. In addition, because simple *in vitro* assays exist for measuring both SOD1's normal function and its abnormal aggregation, we tested whether

side-by-side measurement of both could provide a system for parallel toxicity and efficacy screening of assembly inhibitors and modulators.

## 2 | Materials and methods

### 2.1 | Expression of SOD1 in yeast

Human WT SOD1 was expressed in yeast and purified as described previously (19). Briefly, a recombinant SOD1 plasmid was used to transform EG118 *Saccharomyces cerevisiae* cells, in which the endogenous yeast *sod1* gene is ablated. The expression vectors were cloned previously by the Valentine group, Department of Chemistry and Biochemistry, UCLA, in a YEp-351 plasmid with a LEU2 marker. The cells were transformed using the lithium-acetate method (20) and grown on synthetic defined leucine (SD-Leu) agar media first, and then in liquid media at 30°C. The culture was scaled up in Yeast-Extract Peptone Dextrose (YPD) media (Becton Dickinson) and cells were collected by centrifugation at 4,600 *g* for 10-20 min at 4 °C.

The cell pellet was resuspended in a lysis buffer and SOD1 was purified by sequential chromatography as described previously (19). The collected pure fractions were pooled after measuring SOD1 activity and purity using the XTT assay and SDS-PAGE/Coomassie Blue staining, respectively. One part of pure SOD1 preparation was kept in the metallated form for the enzyme activity assay and the other part was de-metallated for the aggregation assay by stepwise dialysis against: 1) 10 mM EDTA, 100 mM sodium acetate, pH 3.8; 2) 100 mM NaCl, 100 mM sodium acetate, pH 3.8; and 3) 10 mM potassium phosphate, pH 7.0. De-metallated and metallated forms of purified SOD1 were aliquoted and flash frozen for storage at -80°C until further use.

## 2.2 | Compounds

Fifteen compounds were chosen for testing (Figure 3). Ten compounds were chosen because they were reported previously to inhibit the aggregation of other amyloidogenic

proteins and to our knowledge, their inhibition of SOD1 aggregation or activity has not been studied previously. Five additional compounds were chosen due to their reported or proposed inhibition of SOD1 activity and their impact on SOD1 aggregation has not been studied previously. All the

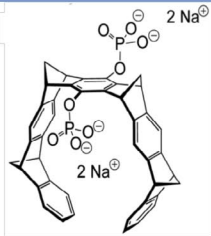
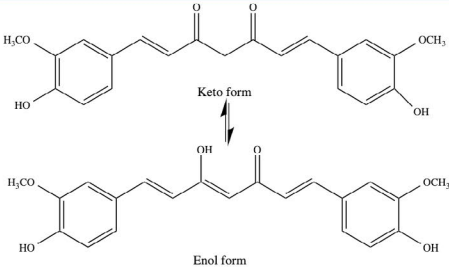
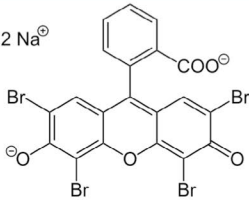
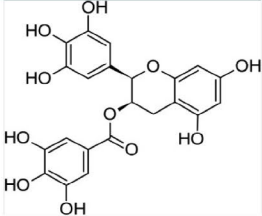
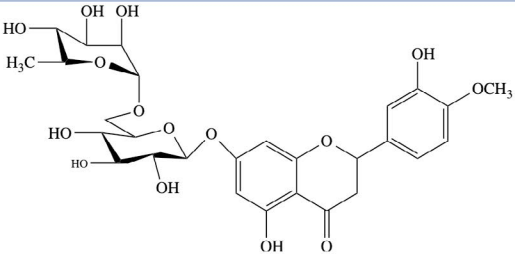
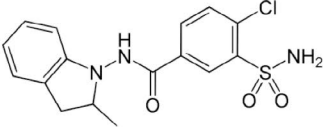
Compound	Structure	Reporter aggregation inhibitor of	References
CLR01		A $\beta$ , $\alpha$ -synuclein, tau, transthyretin, IAPP	(39)
Curcumin		A $\beta$ , $\alpha$ -synuclein, tau	(45), (46), (47)
Eosin Y		A $\beta$	(48), (49)
Epigallocatechin gallate (EGCG)		A $\beta$ , $\alpha$ -synuclein	(50), (51), (52)
Hesperidin		A $\beta$ , tau, $\alpha$ -synuclein, synphilin-1	(53)
Indapamide		Thrombin, A $\beta$	(54) (55)

FIGURE 3 Compounds selected for screening as inhibitors of SOD1 aggregation and enzymatic activity.

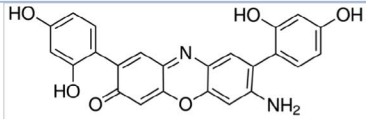
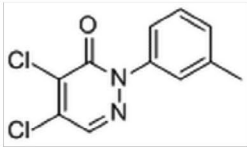
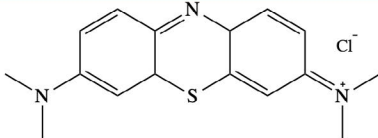
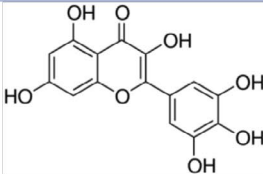
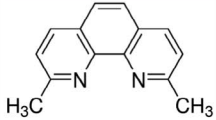
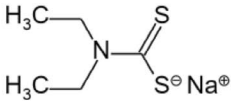
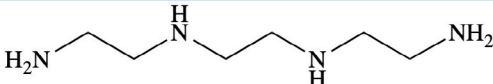
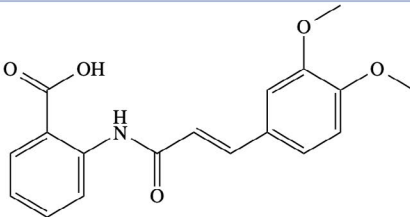
<b>Lacmoid</b>		$\alpha$ -synuclein	(56), (57)
<b>Lung cancer screen 1 (LCS-1)</b>		None	(31)
<b>Methylene blue</b>		Huntingtin, Tar DNA binding protein 43, tau	(58), (59)
<b>Myricetin</b>		Tau, islet amyloid polypeptide (IAPP)	(45), (60), (61)
<b>Neocuproine</b>		A $\beta$	(62), (48)
<b>Potassium Cyanide (KCN)</b>	$K^+ C \equiv N^-$	None	(63)
<b>Sodium diethyldithiocarbamate (DDC)</b>		None	(42)
<b>Triethylenetetramine tetrahydrochloride (TETC)</b>		None	(32)
<b>Tranilast</b>		A $\beta$	(64), (65)

FIGURE 3 Continued

compounds (Figure 3) were obtained from Sigma-Aldrich except for CLR01, which was prepared as described previously (21).

### 2.3 | Thioflavin T (ThT) Fluorescence Assay

De-metallated SOD1 was used for the aggregation assay as in this form SOD1 can easily be induced to aggregate by

reducing its disulfide bonds (22-24). SOD1 was incubated at a concentration of 40  $\mu$ M in the absence or presence of 0.3, 1, 3, or 10 molar equivalents of each compound in 10 mM potassium phosphate, pH 7.4, containing 40  $\mu$ M ThT and 50 mM Tris(2-carboxyethyl)phosphine (TCEP) in a final volume of 100  $\mu$ L (19). The aggregation assay was carried out in 96-well, opaque-walls, clear flat-bottom wells, each containing a Teflon ball to assist with agitation. Triplicate samples were incubated at 37°C with agitation at 300 rpm in



a Synergy HTX plate reader (BioTek Instruments) in three independent experiments. ThT fluorescence was measured every 15 minutes using  $\lambda_{\text{ex}} = 420 \text{ nm}$  and  $\lambda_{\text{em}} = 485 \text{ nm}$  for

48 h. Positive controls excluded the compounds and negative controls excluded SOD1 at each concentration. SOD1 aggregation was normalized to the positive control where no

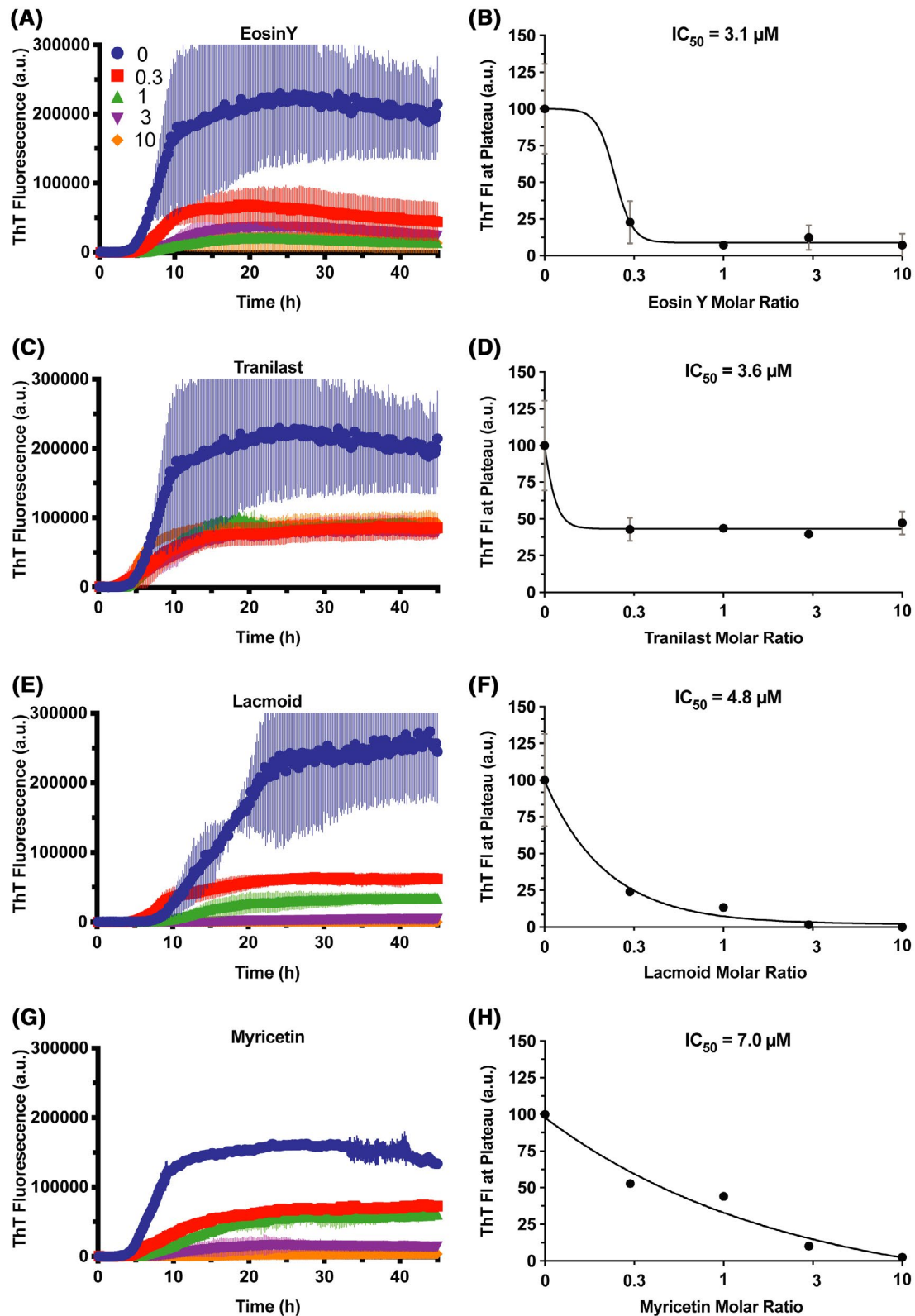


**FIGURE 4** Dose-response analysis of strong inhibitors. ThT fluorescence curves in the presence of increasing concentrations of A) eosin Y, C) tranilast, E) lacmoid, and G) myricetin are shown as mean  $\pm$  SEM of 3 independent experiment each done in 3 technical replicates. Curve fitting using nonlinear regression is shown in panels, B, D, F, and H, respectively.

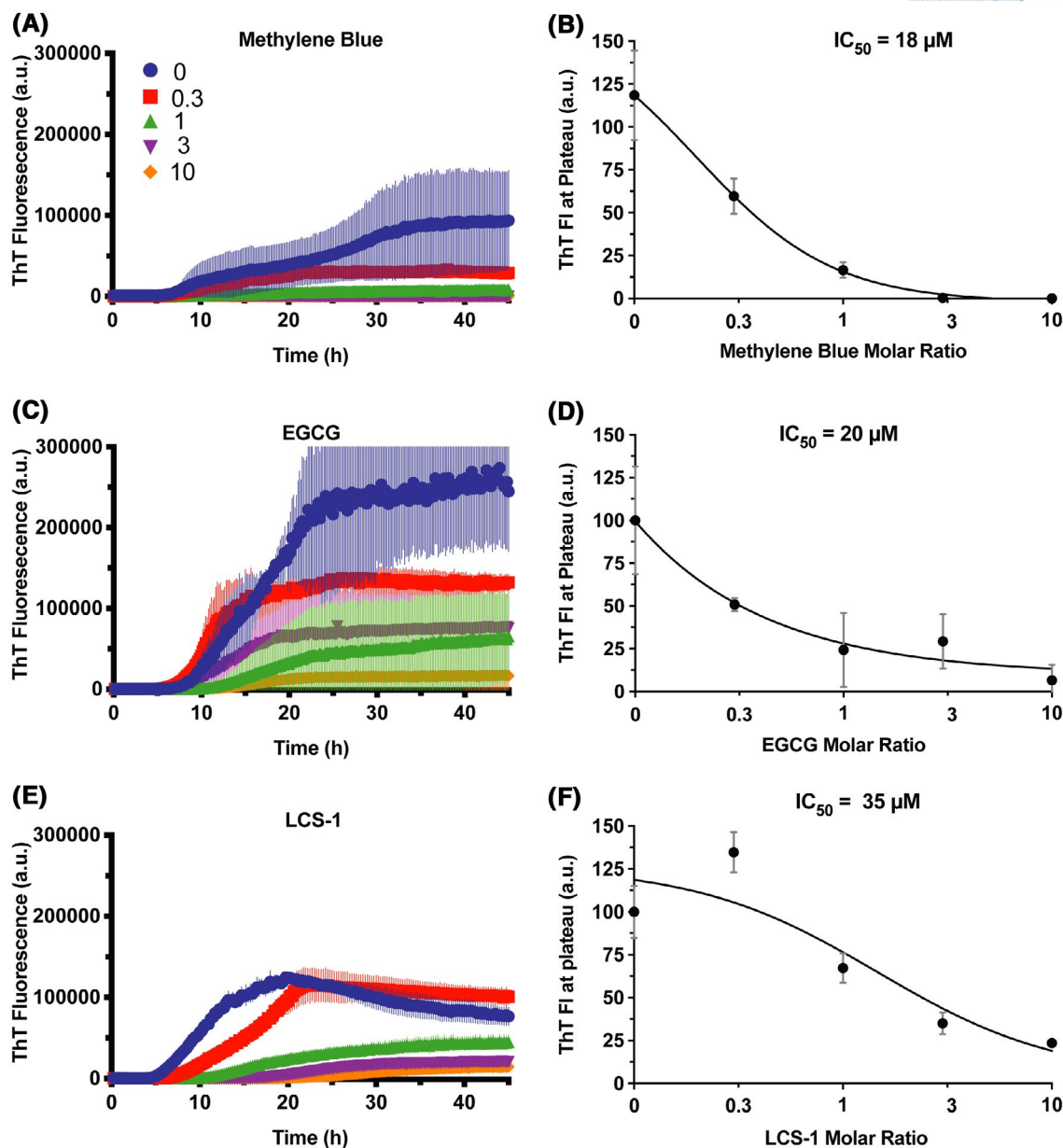


**FIGURE 5** Dose-response analysis of the second group of strong inhibitors. ThT fluorescence curves in the presence of increasing concentrations of A) methylene blue, C) EGCG, and E) LCS-1 are shown as mean  $\pm$  SEM of 3 independent experiment each done in 3 technical replicates. Curve fitting using nonlinear regression is shown in panels, B, D, and F, respectively.

compound was added and considered 100%. Lag times were determined quantitatively using R. We devised an algorithm that measures the slope using 5 consecutive data points at a time. If the slope using the first 5 points did not diverge from 0 ( $p > 0.05$ ), the next set of 5 points (ie, 2 to 6) were used and so on. The last point in which the slope did not diverge from 0 was determined as the lag time and the next point as the beginning of the slope. Plateau values were calculated by averaging the final ten fluorescence values. Maximum velocity was determined by calculating the first derivative of the graph and extracting the maximum value. Data were analyzed in Prism 8.3.0 (GraphPad) by using nonlinear regression and four-parameter curve fitting.

## 2.4 | SOD1 Enzymatic Activity Assay

We used purified, fully metallated SOD1 as the metal co-factors are required for the enzymatic activity of the protein (25,26). The enzymatic activity of SOD1 was analyzed using 7.5 nM of the enzyme. The reaction mixture consisted of 4.92 mM hypoxanthine, 7.5 nM xanthine oxidase, 2.28 nM catalase, 2.42 mM XTT and increasing concentrations of all compounds up to 10,000-fold excess in phosphate-buffered saline, pH 7.2, in a final volume of 325  $\mu$ L except, lung cancer screen 1 (LCS-1) and triethylenetetramine tetrahydrochloride (TETC), which were tested up to 1,000,000-fold excess. Samples were incubated in clear-walled, flat-bottom,

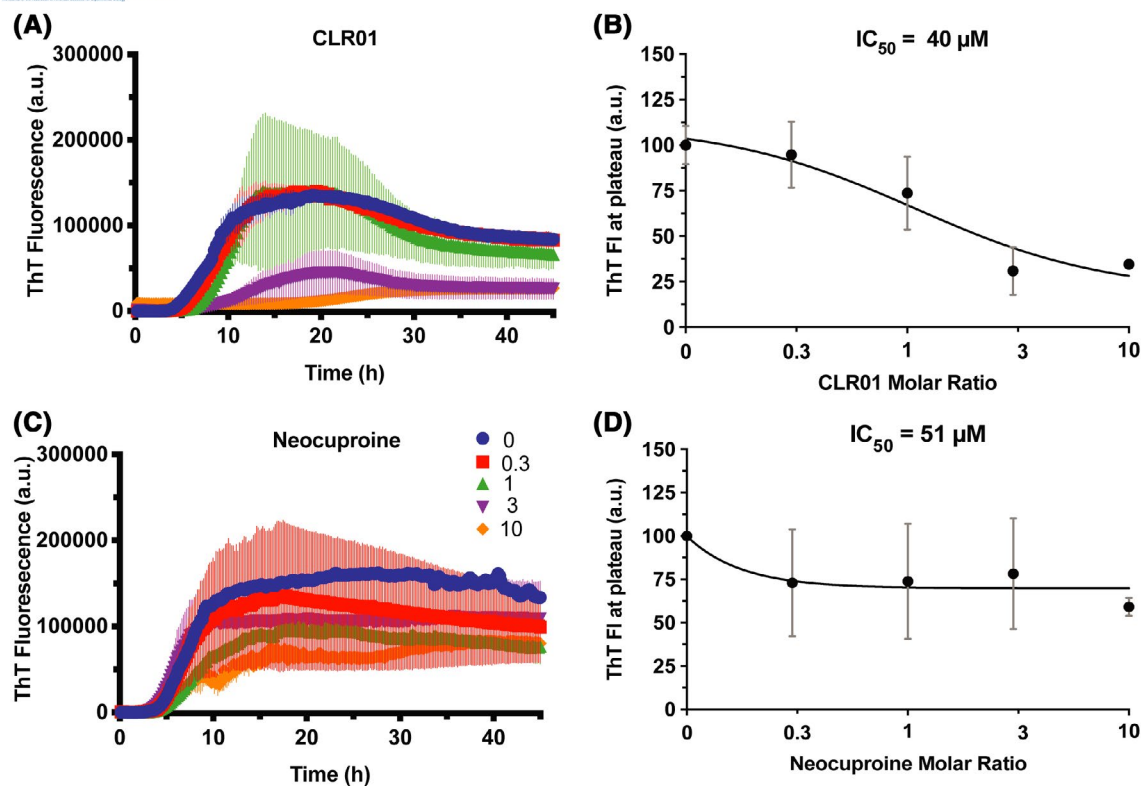


**FIGURE 6** Dose-response analysis of moderate inhibitors. ThT fluorescence curves in the presence of increasing concentrations of A) CLR01 and C) neocuproine are shown as mean  $\pm$  SEM of 3 independent experiment each done in 3 technical replicates. Curve fitting using nonlinear regression is shown in panels, B and D, respectively.

96-well plates for 2 hours at 25°C. The absorbance of the formazan dye was monitored at  $\lambda = 490$  nm every 30 s in a VERSAmax microplate reader (Molecular Devices). Each reaction was monitored in three independent biological replicates, each done in triplicate. Enzymatic activity was determined by analyzing the initial rate of enzyme reaction in each condition by conversion of absorbance values per time to initial enzymatic-activity rate using R (27). The initial rate was calculated by fitting a linear regression through the first 50 data points, corresponding to the first 25 minutes of the reaction. The slope was taken as the initial rate, normalized to the positive control, in which no SOD1 was included (0% of original enzymatic activity) and the negative control containing no inhibitor (100% of original enzymatic activity). Plots were generated in Prism 8.3.0 (GraphPad).

## 2.4.1 | Results

### *Inhibition of SOD1 aggregation*

ThT fluorescence increases substantially when the compound becomes quasi-planar upon binding to the cross- $\beta$  structure of amyloid fibrils (28). Therefore, an increase in fibril formation often correlates with an increase in ThT fluorescence. The rate of this increase can be described by a sigmoidal curve characterized by an initial lag phase, followed

by a sharp increase in fluorescence, and a final plateau phase. The initial lag phase typically is interpreted as the time in which aggregation nuclei form. Within the sharp increase, which signifies fibril elongation and/or secondary nucleation (29), the maximum velocity is a convenient way for comparing rates. The final plateau represents the highest value reached where the maximum amount of  $\beta$ -sheet conversion occurred (in some cases, after the fluorescence has reached a plateau, a decrease in ThT fluorescence is observed when fibrils associate laterally, excluding some ThT binding sites). We extracted these three parameters to gain insight into the effect of each compound on SOD1 aggregation and allow a detailed comparison among the compounds. Because unseeded SOD1 aggregation is known to be a stochastic process (15,16,18), we used SOD1 alone as a positive control in every plate for comparison with the reactions in the presence of the different compounds. The  $IC_{50}$  values were calculated using the specific positive control reaction for each compound.

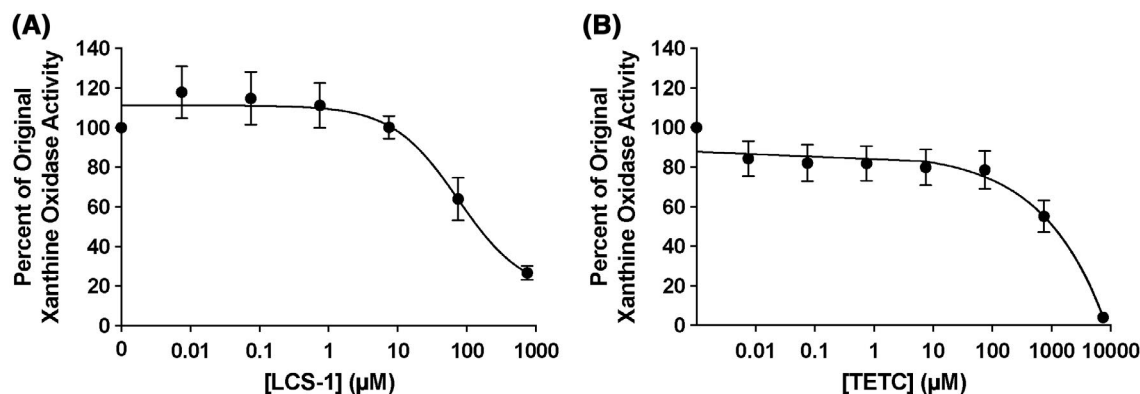
An increase in the lag time and a decrease in the plateau and slope values would signify effective inhibition (19,30). Thus, we calculated the half-maximal inhibitory concentration ( $IC_{50}$ ) for each compound's effect on these three parameters. Because the plateau value is the one typically used in compound screening, we used this value for an initial comparison of the effects of the different compounds, divided them into groups based on the observed  $IC_{50}$ -Plateau values,



**TABLE 1** Inhibition of SOD1 aggregation and activity. IC<sub>50</sub> values were calculated for each parameter separately by non-linear regression using four parameter curves.

Compound	SOD1 aggregation kinetic parameters			Enzyme activity		<i>In-vitro</i> “therapeutic index” (ratio of normalized IC <sub>50</sub> values)
	IC <sub>50</sub> lag time (μM)	IC <sub>50</sub> slope (μM)	IC <sub>50</sub> plateau (μM)	IC <sub>50</sub> xanthine oxidase (μM)	IC <sub>50</sub> SOD1 (μM)	
CLR01	41 ± 29	8 ± 4	40 ± 26	>75,000	>75,000	>46
Curcumin	62 ± 56	21 ± 14	NE	>75,000	>75,000	>30
Eosin Y	15.2 ± 0.0	2.3 ± 0.9	3.1 ± 1.3	>75,000	>75,000	>123
Epigallocatechin gallate (EGCG)	23 ± 9	3 ± 2	20 ± 10	>75,000	>75,000	>82
Hesperidin	100 ± 26	414 ± 313	NE	>75,000	>75,000	>5
Indapamide	NE	186 ± 113	422 ± 347	>75,000	>75,000	>4
Lacmoid	13 ± 2	4.4 ± 0.8	4.8 ± 1.5	>75,000	>75,000	>144
Lung cancer screen 1 (LCS-1)	92 ± 17	55 ± 48	35 ± 2	229 ± 250	NA	NA
Methylene blue	271 ± 177	26 ± 9	18 ± 11	>75,000	>75,000	>7
Myricetin	7 ± 2	5.4 ± 0.9	7.0 ± 0.9	>75,000	>75,000	>268
Neocuproine	52 ± 44	398 ± 23	51 ± 47	>75,000	>75,000	>5
Potassium cyanide (KCN)	NE	NE	NE	>75,000	39 ± 7	NA
Sodium diethyldithiocarbamate (DDC)	45 ± 26	63 ± 29	NE	>75,000	5.6 ± 0.5	0.002
Triethylenetetramine tetrahydrochloride (TETC)	NE	1767 ± 1551	NE	1036 ± 827	NA	NA
Tranilast	206 ± 141	187 ± 182	3.6 ± 1.8	>75,000	>75,000	>9

The values are shown as mean ± SEM. NA = not applicable, NE = no effect. For calculation of the *in-vitro* “therapeutic index” (TI) the half-maximal inhibitory concentration of enzyme activity normalized to the concentration of active SOD1 in the XTT assay was divided by the largest of the three IC<sub>50</sub> values for SOD1 aggregation normalized to the concentration of de-metallated SOD1 in the ThT-fluorescence assay.

**FIGURE 7** LCS-1 and TETC inhibit xanthine oxidase. A) LCS-1 or B) TETC were added to the XTT assay system in the absence of SOD1 in three independent experiments, each done in three technical replicates. The data are presented as mean ± SEM.

and then, asked how the other two parameters, IC<sub>50-Lag time</sub> and IC<sub>50-Slope</sub> compared with the IC<sub>50-Plateau</sub>. Compounds for which the IC<sub>50-Plateau</sub> values were below the concentration of SOD1 used in the experiments, 40 μM, were considered strong inhibitors (Figures 3,4). Those with IC<sub>50-Plateau</sub> values between 40 and 80 μM were considered moderate (Figure 6), and compounds with higher IC<sub>50-Plateau</sub> were defined as weak inhibitors (Supplementary Figure S1). Dose-response curves

are shown only for the IC<sub>50-Plateau</sub>, whereas the values of the three parameters for all the compounds are summarized in Table 1.

The strongest inhibitors based on the plateau values were eosin Y (Figure 4A), IC<sub>50-Plateau</sub> = 3.1 ± 1.3 μM (Figure 4B), tranilast (Figure 4C)—3.6 ± 1.8 μM (Figure 4D), lacmoid (Figure 4E)—4.8 ± 1.5 μM (Figure 4F), and myricetin (Figure 4G)—7.0 ± 0.9 μM (Figure 4H). However, although the

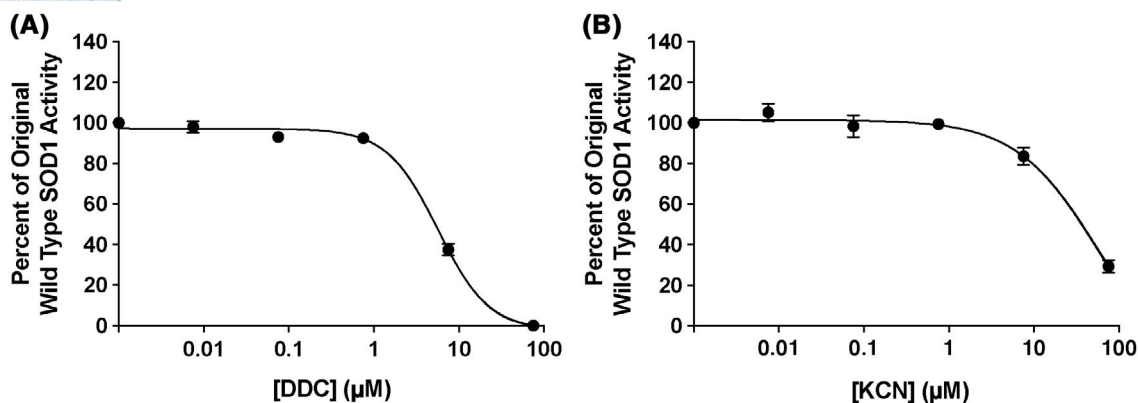


**FIGURE 8** Inhibition of SOD1 enzymatic activity by DDC and KCN. A) DDC or B) KCN were added to the XTT assay system in three independent experiments, each done in three technical replicates. The data are presented as mean  $\pm$  SEM.

$IC_{50}$  values of these compounds were close, examination of the dose-response curves showed that they displayed distinct behaviors. Eosin Y and lacmoid decreased the plateau values sharply already at the lowest concentration used, 12  $\mu$ M (corresponding to a compound:SOD1 molar ratio = 0.3) followed by a more gradual decrease (Figure 4B,F), whereas the effect of myricetin was gradual throughout the concentration range used (Figure 4H). Peculiarly, tranilast decreased the plateau value sharply at a tranilast:SOD1 concentration ratio = 0.3 to ~50% the control value but no further decrease was observed at higher concentrations (Figure 4D). Myricetin had the strongest impact on the lag time,  $IC_{50-Lag\ time} = 5.4 \pm 0.9 \mu$ M, suggesting that it inhibited strongly the nucleation step in SOD1 aggregation. Lacmoid and Eosin Y also were relatively strong inhibitors of the nucleation step, with  $IC_{50-Lag\ time} = 13 \pm 2$  and  $15.2 \pm 0$ , respectively, whereas tranilast was a weak inhibitor of the lag phase,  $IC_{50-Lag\ time} = 206 \pm 141 \mu$ M. Tranilast also had a weak effect on the exponential increase phase,  $IC_{50-Slope} = 187 \pm 182 \mu$ M, whereas the three other compounds were strong inhibitors (Table 1). These results demonstrated that adding the lag-time and slope analysis of the inhibitors' effect on SOD1 aggregation yields a different picture than analysis of the plateau alone. When all three parameters are considered, myricetin emerges as the strongest inhibitor whereas tranilast appears to be a weak inhibitor, suggesting that its effect on the plateau value would lead to a false-positive result in a typical screen.

In the next group of strong inhibitors, methylene blue (Figure 5A) reduced the plateau value with  $IC_{50-Plateau} = 18 \pm 11 \mu$ M (Figure 5B), epigallocatechin gallate (EGCG, Figure 5C) with  $IC_{50-Plateau} = 20 \pm 10 \mu$ M (Figure 5D), and LCS-1 (Figure 5E) with  $IC_{50-Plateau} = 35 \pm 2 \mu$ M (Figure 5F). All three compounds showed a gradual decrease in the ThT-fluorescence plateau value across the concentration range used (Figure 5). EGCG also showed strong effects on the lag time ( $IC_{50-Lag\ time} = 23 \pm 9 \mu$ M) and particularly on the slope ( $IC_{50-Slope} = 3 \pm 2 \mu$ M), whereas methylene blue inhibited the slope with  $IC_{50-Slope} = 26 \pm 9 \mu$ M but had a weak impact on the lag time ( $IC_{50-Lag\ time} = 271 \pm 177$ ), suggesting that it affected primarily the

elongation of SOD1 fibrils but not the nucleation step. LCS-1 was a moderate inhibitor of the slope ( $IC_{50-Slope} = 55 \pm 48 \mu$ M) and a weak inhibitor of SOD1 nucleation ( $IC_{50-Lag\ time} = 92 \pm 17 \mu$ M). Considering all three parameters, EGCG appeared to be the strongest inhibitor in this group, despite having a higher  $IC_{50-Plateau}$  value than methylene blue.

The moderate-inhibitor group included CLR01 (Figure 6A) and neocuproine (Figure 6C), which showed  $IC_{50-Plateau}$  values of  $40 \pm 26 \mu$ M and  $51 \pm 47 \mu$ M, respectively (Figure 5B,D). Both compounds also had moderate effects on the lag time,  $IC_{50-Lag\ time} = 41 \pm 29 \mu$ M and  $52 \pm 44 \mu$ M, respectively. However, unlike neocuproine, which had a weak effect on the slope ( $IC_{50-Slope} = 398 \pm 23 \mu$ M), CLR01 showed strong inhibition of the slope ( $IC_{50-Slope} = 8.3 \pm 4.3 \mu$ M), suggesting that its main effect was on SOD1 elongation and/or secondary nucleation.

In the weak-inhibitors group, curcumin, sodium diethyldithiocarbamate (DDC), hesperidin, indapamide, KCN, and TETC did not affect the ThT fluorescence plateau meaningfully up to 10-fold excess (Supplementary Figure S1). However, two of these compounds, curcumin ( $IC_{50-Lag\ time} = 62 \pm 56 \mu$ M,  $IC_{50-Slope} = 21 \pm 14 \mu$ M) and DDC ( $IC_{50-Lag\ time} = 45 \pm 26 \mu$ M,  $IC_{50-Slope} = 63 \pm 29 \mu$ M), had moderate effects on the lag time and slope, demonstrating that these compounds would yield false-negative results in a screen based only on the plateau values.

#### *Inhibition of SOD1 enzymatic activity*

The assay system we used for measuring SOD1 activity depends on generation of superoxide radical anions from hypoxanthine by xanthine oxidase. Therefore, if a compound included in the screen inhibits xanthine oxidase, it would lead to a false-positive readout because no formazan would be formed. To address this potential issue, we tested each compound first as a pre-screen in the absence of SOD1 to determine if it inhibited xanthine oxidase. Interestingly, we found that two compounds reported previously to inhibit SOD1 activity, LCS-1 (31) and TETC (32), actually inhibited

xanthine oxidase. LCS-1 inhibited xanthine oxidase,  $IC_{50} = 229 \pm 144 \mu\text{M}$  whereas TETC was a weaker inhibitor,  $IC_{50} = 1036 \pm 477 \mu\text{M}$  (Figure 7). No other compound was found to affect xanthine oxidase when tested at concentrations up to  $10^4$ -fold excess relative to the enzyme (data not shown). Thus, our pre-screen results suggest that the previous reports likely were incorrect, reflecting inhibition of xanthine oxidase rather than of SOD1. In light of these findings, LCS-1 and TETC were excluded from subsequent experiments testing inhibition of SOD1 activity.

Testing all the other compounds for inhibition of SOD1 enzymatic activity, we found that DDC and KCN inhibited the enzymatic activity of SOD1 with  $IC_{50}$  values of  $5.6 \pm 0.5$  and  $38.6 \pm 7.3 \mu\text{M}$ , respectively (Figure 8), consistent with previous reports (33,34). No other compound affected the activity of SOD1 up to the highest concentration, suggesting that if these compounds inhibited SOD1 aggregation efficiently they would be safe based on the *in vitro* screen. At the same time, the inability of *any* aggregation inhibitor to reduce SOD1 activity at all suggests that SOD1 is not suitable for assessment of safety *in vitro* due to a very high resistance to inhibition by diverse compounds.

## 2.4.2 | Discussion

Aberrant protein aggregation is involved in over 50 proteinopathies affecting millions of people worldwide yet very few disease-modifying therapies exist to target them (2). Most drug candidates fail due to low efficacy or side effects. Therefore, improved methods for drug discovery and development are needed. Here, we tested a strategy for directly assessing aggregation inhibition and potential toxicity of compounds *in vitro* utilizing the readily available, simple assays for measuring SOD1 aggregation and activity. We aimed to calculate an *in vitro* equivalent of a “therapeutic index” for the screened compounds that could serve as a basis for comparison later in cell culture and/or animal experiments. Because the concentrations of SOD1 used for the aggregation and enzymatic activity assays differed by  $>3$  orders of magnitude, which was based on the sensitivity of the assays, for the calculation of the “therapeutic index”, the  $IC_{50}$  values were normalized to the SOD1 concentration in each assay.

Few aggregation inhibitors have been tested against SOD1 to date (19). FDA-approved drugs were screened *in vitro* using turbidity and electrophoresis, which identified a few classes of inhibitors (35), yet, mechanistic details are not available. In our study, we used the ThT-fluorescence assay to test aggregation inhibitors reported previously for other amyloidogenic proteins but not for SOD1. We found that many of them indeed inhibited SOD1 aggregation (Figures 3-5), supporting the notion that such compounds are not specific to one protein

(36,37). Our data also revealed that different compounds affect different stages of the aggregation reaction (38).

The maximal ThT fluorescence is used commonly for screening of aggregation inhibitors, whereas the kinetics of the reaction often is neglected in such screens. However, our data demonstrate that using only the maximal fluorescence can be misleading, yielding both false-positive and false-negative results (Table 1). For example, based on our results, tranilast (Figure 4C,D) would yield a false-positive hit, whereas curcumin would give a false-negative result (Table 1).

The data also point to different mechanisms by which compounds might inhibit SOD1 aggregation. For example, myricetin, lacmoid, eosin Y and EGCG extended the lag time substantially at substoichiometric concentrations relative to SOD1 and reduced the slope, suggesting that they can both attenuate the nucleation step and suppress fibril elongation, whereas CLR01, curcumin, and methylene blue affected predominantly the elongation/secondary nucleation phase (Table 1). We note that CLR01 likely acts by a distinct mechanism from the polyphenols and similar compounds studied here. CLR01 binds specifically to Lys residues with low micromolar affinity and with 5-10-fold lower affinity to Arg residues. The binding is highly labile and disrupts the self-assembly process by perturbing both hydrophobic and electrostatic interactions (39). Previously, we have shown that the compound inhibits effectively the aggregation of WT and variant SOD1 both *in vitro* and in a mouse model (19). In contrast, the binding sites of polyphenols and other aggregation inhibitors are not well defined and some may actually bind covalently to primary amino groups, such as those of Lys residues and/or the amino terminus (40,41). In view of these different mechanisms, it is not clear to what extent the simple comparison of the inhibitory activity in the ThT assay can be used to compare CLR01 with the other compounds.

Of the compounds selected for their reported or predicted ability to inhibit SOD1 enzymatic activity, both DDC and LCS-1 were found to have aggregation-inhibition activity. In the case of LCS-1 this activity likely is mediated by the aromatic groups, whereas the mechanism by which DDC inhibits aggregation is not known. Because LCS-1 was found to be an inhibitor of xanthine oxidase, it could not be evaluated for inhibition of SOD1 in our system, and thus, we could not estimate its *in vitro* therapeutic index. The *in vitro* therapeutic index for DDC was found to be 0.002, which means that the compound is too toxic to be used as an aggregation inhibitor.

None of the aggregation inhibitors affected enzymatic activity of SOD1. Therefore, we listed relatively high *in vitro* therapeutic indexes for these compounds in Table 1, though these values should be taken with a grain of salt because inhibitor activity was quantified by means of  $IC_{50}$  values in both assays for only one compound, DDC, which is a copper chelator and a known inhibitor of SOD1 activity.

The only other inhibitor of SOD1 activity, KCN, which is a potent poison, was inactive as an aggregation inhibitor.

The inhibition of SOD1 activity by DDC was in agreement with previous reports (42) and computational modeling (43). DDC and CN<sup>-</sup> are negatively charged, and therefore, are more likely to bind to the active site of SOD1 than neutral molecules, for example, hesperidin (44). A three-dimensional electrostatic vector field analysis of SOD1 showed that the highly positively charged active site attracts negatively charged molecules for catalysis (44), providing insight into the mechanism of action of negatively charged inhibitors.

When attempting to reproduce previously reported results with LCS-1 (31) and TETC (32), we found that both compounds actually inhibited xanthine oxidase leading to a false-positive result for inhibition of SOD1. As neither previous study reported tested these compounds in control reactions excluding SOD1, we suspect that their observations likely were a misinterpretation of the inhibition of xanthine oxidase as inhibition of SOD1, highlighting the importance of testing compounds for inhibition of both enzymes in the assay.

In summary, our results suggest that conducting screens for aggregation inhibitors using the maximal fluorescence values in ThT-fluorescence assays is likely to produce false-positive and false-negative results that can be avoided if the kinetic curves are monitored and the lag time and slope are also analyzed. Using this approach, we found that eosin Y, EGCG, lacmoid, and myricetin are potent inhibitors of SOD1 aggregation and identified several other compounds with somewhat lower activity. We observed that different compounds have distinct impacts on the lag phase, slope, and plateau of the ThT fluorescence. However, though we hoped that parallel assays of SOD1 activity and aggregation could generate an informative therapeutic index estimation in vitro, the results show that the system cannot fulfill this premise because SOD1 is resistant to inhibition by most compounds.

## ACKNOWLEDGMENTS

The work was supported by NIH/NIA R01 grant AG050721 and RGK Foundation grant 20143057. We thank Dr. Joan Valentine for the SOD1 plasmids.

## CONFLICTS OF INTEREST

The authors declare no conflict of interest

## AUTHOR CONTRIBUTIONS

RM and CC performed the experiments, interpreted the data, and wrote the manuscript, ML compiled an initial list of compounds and performed preliminary testing, HA performed thioflavin T experiment, NS produced SOD1, GB supervised the project, wrote the manuscript, and acquired funding.

## REFERENCES

- Eisele YS, Monteiro C, Fearn C, et al. Targeting protein aggregation for the treatment of degenerative diseases. *Nat Rev Drug Discov.* 2015;14:759–780.
- Bitan G. Disease-modifying therapy for proteinopathies: Can the exception become the rule? *Prog Mol Biol Transl Sci.* 2019;168:277–287.
- Sangwan S, Zhao A, Adams KL, et al. Atomic structure of a toxic, oligomeric segment of SOD1 linked to amyotrophic lateral sclerosis (ALS). *Proc. Natl. Acad. Sci. USA.* 2017;114:8770–8775.
- Liu T, Bitan G. Modulating self-assembly of amyloidogenic proteins as a therapeutic approach for neurodegenerative diseases: strategies and mechanisms. *ChemMedChem.* 2012;7:359–374.
- Rahimi F, Li H, Sinha S, Bitan G. Modulators of Amyloid  $\beta$ -Protein (A $\beta$ ) Self-Assembly. In: Wolfe MS, ed. *Developing Therapeutics for Alzheimer's Disease.* Boston: Academic Press; 2016:97–191.
- Gurney M, Pu H, Chiu A, et al. Motor neuron degeneration in mice that express a human Cu, Zn superoxide dismutase mutation. *Science.* 1994;264:1772–1775.
- Bunton-Stasyshyn RK, Saccon RA, Fratta P, Fisher EM. SOD1 Function and Its Implications for Amyotrophic Lateral Sclerosis Pathology: New and Renascent Themes. *Neuroscientist.* 2015;21:519–529.
- Sakellariou GK, McDonagh B, Porter H, et al. Comparison of Whole Body SOD1 Knockout with Muscle-Specific SOD1 Knockout Mice Reveals a Role for Nerve Redox Signaling in Regulation of Degenerative Pathways in Skeletal Muscle. *Antioxid Redox Signal.* 2018;28:275–295.
- Sehati S, Clement MH, Martins J, et al. Metabolic alterations in yeast lacking copper-zinc superoxide dismutase. *Free Radic Biol Med.* 2011;50:1591–1598.
- Flora G, Gupta D, Tiwari A. Toxicity of lead: A review with recent updates. *Interdiscip Toxicol.* 2012;5:47–58.
- Sutherland MW, Learmonth BA. The tetrazolium dyes MTS and XTT provide new quantitative assays for superoxide and superoxide dismutase. *Free Radic Res.* 1997;27:283–289.
- Cantu-Medellin N, Kelley EE. Xanthine oxidoreductase-catalyzed reactive species generation: A process in critical need of reevaluation. *Redox Biol.* 2013;1:353–358.
- Rodriguez JA, Valentine JS, Eggers DK, et al. Familial amyotrophic lateral sclerosis-associated mutations decrease the thermal stability of distinctly metallated species of human copper/zinc superoxide dismutase. *J. Biol. Chem.* 2002;277:15932–15937.
- Naiki H, Higuchi K, Hosokawa M, Takeda T. Fluorometric determination of amyloid fibrils in vitro using the fluorescent dye, thioflavin T1. *Anal Biochem.* 1989;177:244–249.
- Abdolvahabi A, Shi Y, Rasouli S, et al. Kaplan-Meier Meets Chemical Kinetics: Intrinsic Rate of SOD1 Amyloidogenesis Decreased by Subset of ALS Mutations and Cannot Fully Explain Age of Disease Onset. *ACS Chem. Neurosci.* 2017;8:1378–1389.
- Abdolvahabi A, Shi Y, Chuprin A, Rasouli S, Shaw BF. Stochastic Formation of Fibrillar and Amorphous Superoxide Dismutase Oligomers Linked to Amyotrophic Lateral Sclerosis. *ACS Chem. Neurosci.* 2016;7:799–810.
- Atlasi RS, Malik R, Corrales CI, et al. Investigation of Anti-SOD1 Antibodies Yields New Structural Insight into SOD1 Misfolding and Surprising Behavior of the Antibodies Themselves. *ACS Chem. Biol.* 2018;13:2794–2807.



18. Lang L, Zetterstrom P, Brannstrom T, Marklund SL, Danielsson J, Oliveberg M. SOD1 aggregation in ALS mice shows simplistic test tube behavior. *Proc. Natl. Acad. Sci. USA.* 2015;112:9878–9883.
19. Malik R, Meng H, Wongkongkathep P, et al. The molecular tweezer CLR01 inhibits aberrant superoxide dismutase 1 (SOD1) self-assembly in vitro and in the G93A-SOD1 mouse model of ALS. *J. Biol. Chem.* 2019;294:3501–3513.
20. Gietz RD, Woods RA. Transformation of yeast by lithium acetate/single-stranded carrier DNA/polyethylene glycol method. *Methods Enzymol.* 2002;350:87–96.
21. Talbiersky P, Bastkowski F, Klärner FG, Schrader T. Molecular clip and tweezer introduce new mechanisms of enzyme inhibition. *J. Am. Chem. Soc.* 2008;130:9824–9828.
22. Doucette PA, Whitson LJ, Cao X, et al. Dissociation of human copper-zinc superoxide dismutase dimers using chaotrope and reductant. Insights into the molecular basis for dimer stability. *J. Biol. Chem.* 2004;279:54558–54566.
23. Chattopadhyay M, Durazo A, Sohn SH, et al. Initiation and elongation in fibrillation of ALS-linked superoxide dismutase. *Proc. Natl. Acad. Sci. USA.* 2008;105:18663–18668.
24. Sheng Y, Chattopadhyay M, Whitelegge J, Valentine JS. SOD1 aggregation and ALS: role of metallation states and disulfide status. *Curr Top Med Chem.* 2012;12:2560–2572.
25. Toichi K, Yamanaka K, Furukawa Y. Disulfide scrambling describes the oligomer formation of superoxide dismutase (SOD1) proteins in the familial form of amyotrophic lateral sclerosis. *J. Biol. Chem.* 2013;288:4970–4980.
26. Tokuda E, Nomura T, Ohara S, et al. A copper-deficient form of mutant Cu/Zn-superoxide dismutase as an early pathological species in amyotrophic lateral sclerosis. *Biochim Biophys Acta Mol Basis Dis.* 2018;1864:2119–2130.
27. Core Team R. *R: A language and environment for statistical computing.* Vienna, Austria: R Foundation for Statistical Computing; 2013. <http://www.R-project.org/>.
28. Biancalana M, Koide S. Molecular mechanism of Thioflavin-T binding to amyloid fibrils. *Biochim. Biophys. Acta.* 2010;1804:1405–1412.
29. Knowles TP, Waudby CA, Devlin GL, et al. An analytical solution to the kinetics of breakable filament assembly. *Science.* 2009;326:1533–1537.
30. Metrick MA, do Carmo Ferreira N, Saijo E, et al. Million-fold sensitivity enhancement in proteopathic seed amplification assays for biospecimens by Hofmeister ion comparisons. *Proc. Natl. Acad. Sci. USA.* 2019;116:23029–23039.
31. Somwar R, Erdjument-Bromage H, Larsson E, et al. Superoxide dismutase 1 (SOD1) is a target for a small molecule identified in a screen for inhibitors of the growth of lung adenocarcinoma cell lines. *Proc. Natl. Acad. Sci. USA.* 2011;108:16375–16380.
32. Weissmann N, Tadic A, Hanze J, et al. Hypoxic vasoconstriction in intact lungs: a role for NADPH oxidase-derived H(2)O(2)? *Am J Physiol Lung Cell Mol Physiol.* 2000;279:L683–690.
33. Zolnierowicz S, Zelewski M, Swierczynski J, Marszalek J, Zelewski L. Cyanide—an uncompetitive inhibitor of NAD(P)-dependent malic enzyme from human term placental mitochondria. *Biochem Int.* 1988;17:303–309.
34. Brennan RE, Kiss K, Baalman R, Samuel JE. Cloning, expression, and characterization of a Coxiella burnetii Cu/Zn Superoxide dismutase. *BMC Microbiol.* 2015;15:99.
35. Anzai I, Toichi K, Tokuda E, Mukaiyama A, Akiyama S, Furukawa Y. Screening of Drugs Inhibiting In vitro Oligomerization of Cu/Zn-Superoxide Dismutase with a Mutation Causing Amyotrophic Lateral Sclerosis. *Front Mol Biosci.* 2016;3:40.
36. Sweeney P, Park H, Baumann M, et al. Protein misfolding in neurodegenerative diseases: implications and strategies. *Transl Neurodegener.* 2017;6:6.
37. Andrich K, Bieschke J. The Effect of (-)-Epigallo-catechin-(3)-gallate on Amyloidogenic Proteins Suggests a Common Mechanism. *Adv Exp Med Biol.* 2015;863:139–161.
38. Metrick MA 2nd, Ferreira NDC, Saijo E, et al. A single ultrasensitive assay for detection and discrimination of tau aggregates of Alzheimer and Pick diseases. *Acta Neuropathol. Commun.* 2020;8:22.
39. Schrader T, Bitan G, Klärner FG. Molecular tweezers for lysine and arginine - powerful inhibitors of pathologic protein aggregation. *Chem Commun (Camb).* 2016;52:11318–11334.
40. Palhano FL, Lee J, Grimster NP, Kelly JW. Toward the molecular mechanism(s) by which EGCG treatment remodels mature amyloid fibrils. *J. Am. Chem. Soc.* 2013;135:7503–7510.
41. Sato M, Murakami K, Uno M, et al. Site-specific inhibitory mechanism for amyloid  $\beta$ 42 aggregation by catechol-type flavonoids targeting the Lys residues. *J. Biol. Chem.* 2013;288:23212–23224.
42. Misra HP. Reaction of copper-zinc superoxide dismutase with diethyldithiocarbamate. *J. Biol. Chem.* 1979;254:11623–11628.
43. Dong X, Zhang Z, Zhao J, et al. The rational design of specific SOD1 inhibitors via copper coordination and their application in ROS signaling research. *Chem Sci.* 2016;7:6251–6262.
44. Getzoff ED, Tainer JA, Weiner PK, Kollman PA, Richardson JS, Richardson DC. Electrostatic recognition between superoxide and copper, zinc superoxide dismutase. *Nature.* 1983;306:287–290.

## SUPPORTING INFORMATION

Additional Supporting Information may be found online in the Supporting Information section.

**How to cite this article:** Malik R, Corrales C, Linsenmeier M, Alalami H, Sepanj N, Bitan G. Examination of SOD1 aggregation modulators and their effect on SOD1 enzymatic activity as a proxy for potential toxicity. *The FASEB Journal.* 2020;34:11957–11969. <https://doi.org/10.1096/fj.202000948R>